entire ensemble is affected immediately. In the steady state, however, only a portion of the molecules are in the signal generating portion of the photocycle.

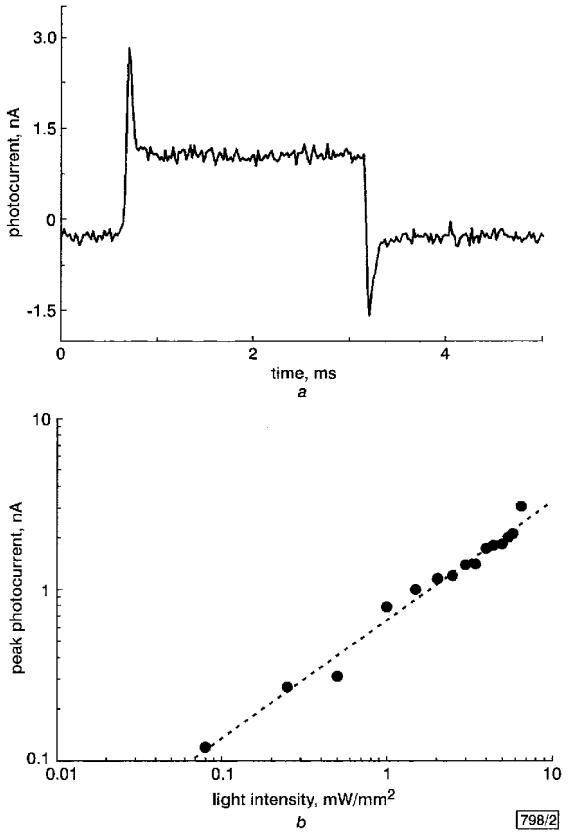

Fig. 2 *Measured photoresponse waveform to modulated 630nm light for conduction across ITO/bR/Au/GaAs under ambient humidity conditions and peak photocurrent across sample as function of incident light intensity*

a Photoresponse waveform
Light intensity = 8mW/mm^2
b Peak photocurrent against incident light intensity

The effect of aging of the bR is not revealed in our experiments. This is because the photoexcitation has a wavelength (632nm) that is significantly different from the absorption peak wavelength (570nm) of the bR molecule. This results in a small absorption by the bR film and a small number of molecules being converted to the M photointermediate state, which does not seriously lower the total available population of the bR ground state.

Acknowledgment: This work is supported by the Army Research Office (MURI program) under Grant DAAD19-99-1-0198. Discussions with S. Datta and D. Janes are gratefully acknowledged.

16 October 2000
Electronics Letters Online No: 20010426
DOI: 10.1049/el:20010426

J. Xu and P. Bhattacharya (*Solid State Electronics Laboratory, Department of Electrical Engineering and Computer Science, University of Michigan, Ann Arbor, MI 48109-2122, USA*)

E-mail: pkb@eecs.umich.edu

D.L. Marcy, J.A. Stuart and R.R. Birge (*W.M. Keck Center for Molecular Electronics & Department of Chemistry, Syracuse University, Syracuse, NY 13244, USA*)

R.R. Birge: Present address: Department of Chemistry and Molecular & Cell Biology, University of Connecticut, Storrs, CT 06269, USA

References

1 BIRGE, R.R., GILLESPIE, N.B., IZAGUIRRE, E.W., KUSNETZOW, A., LAWRENCE, A.F., SINGH, D., SONG, Q.W., SCHMIDT, E., STUART, J.A., SEETHARAMAN, S., and WISE, K.J.: 'Biomolecular electronics: protein-based associative processors and volumetric memories', *J. Phys. Chem. B*, 1999, **103**, pp. 10746 10766

2 LOZIER, R.H., BOGOLNI, R.A., and STOECKENIUS, W.: 'Bacteriorhodopsin: a light-driven proton pump in Halobacterium halobium', *Biophys. J.*, 1975, **15**, pp. 955–962

3 BIRGE, R.R., DESHAN, , IZGI, K.C., and TAN, E.H.L.: 'Role of cacium in the proton pump of bacteriorhodopsin. Microwave evidence for a cation-gated mechanism', *J. Phys. Chem.*, 1996, **100**, pp. 9990–10004

4 HONG, F.T.: 'Molecular sensors based on the photoelectric effect of bacteriorhodopsin: origin of differential responsivity', *Mater. Sci. Eng.*, 1997, **4**, pp. 267–285

5 MIYASAKA, T.K., and ITOH, I.: 'Quantum conversion and image detection by a bacteriorhodopsin-based artificial photoreceptor', *Science*, 1992, **255**, pp. 342–344

6 TAKEI, H., LEWIS, A., and NEBENZAHL, I.: 'Implementing receptive fields with excitatory and inhibitory optoelectrical response of bacteriorhodopsin films', *Appl. Opt.*, 1991, **30**, pp. 500–509

7 ROBERTSON, B., and LUKASHEV, F.: 'Rapid pH change due to bacteriorhodopsin measured with a tin-oxide electrode', *Biophys. J.*, 1995, **68**, pp. 1507–1517

8 KONONENKO, A.A., CHAMOROVKSY, S.K., MAXIMYCHEV, A.V., TIMASHEV, S.F., CHEKULAEVA, L.N., and RUBIN, A.B.: 'Oriented purple-membrane film as a probe for studies of the mechanism of bacteriorhodospin functioning II. Photoelectric process', *Biochimica et Biophysica Acta*, 1987, **892**, pp. 56 67

SAR interferometric phase noise reduction using wavelet transform

C.L. Martínez, X.F. Cànovas and M. Chandra

The problem of synthetic aperture radar interferometric phase noise reduction is addressed. A new technique based on discrete wavelet transform is presented. This technique guarantees high resolution phase estimation without using phase image segmentation. Areas containing only noise are hardly processed. Tests with synthetic and real interferograms are reported.

Introduction: Synthetic aperture radar interferometry (InSAR) has been successfully applied to obtain topographic information of the earth's surface. Interferograms are formed multiplying a synthetic aperture radar (SAR) image by the complex conjugate of a second SAR image taken from a slightly different position. The phase of the interferogram at each point is then proportional to its topographic height. Interferometric phase is wrapped in a 2π modulus making it necessary to unwrap the phase to derive topographic information. The degree of coherence between SAR images determines interferometric phase quality. Factors such as system noise, terrain decorrelation (non-simultaneous surveys), image misregistration, geometric decorrelation, act as noise sources. The principal effect of phase noise are residues (phase points with nonzero rotational), as they make the unwrapping process dependent on the path through which the phase is integrated.

To facilitate unwrapping the interferometric phase, it is necessary to remove phase noise. As coherence varies across phase image, phase noise is a non-stationary process. Therefore, any kind of phase noise reduction algorithm has to take into account this non-stationarity. A common way to reduce phase noise is to make use of a coherent averaging or multilook filter. Unfortunately, noise reduction is achieved at the expense of spatial resolution. Other existing techniques always make use of some kind of phase windowing to process it locally. For example, the technique presented in [1] despite outperforming a mean filter, also applies a windowing segmentation process.

In this Letter, we present a new technique to remove SAR interferometric phase noise. This technique is based on discrete wavelet transform (DWT) [2]. The purpose of using DWT is to avoid a phase windowing process, performing a local phase analysis, and therefore, achieving phase noise reduction within the wavelet domain. The algorithm is not based on coefficient thresholding, as we have observed that these techniques present poor results in low coherence areas. The technique also minimises the loss of resolution suffered by techniques using the DWT duality property [2]; in addition, it does not require previous phase unwrapping.

Principle of operation: To maintain phase jumps, which contain information for phase unwrapping, interferometric phase is processed in the complex plane:

$$\hat{\psi} = \arg\{T_\psi(e^{j\psi})\} = \arg\{T_\psi(\Re(e^{j\psi})) + j \cdot T_\psi(\Im(e^{j\psi}))\} \quad (1)$$

where ψ and $\hat{\psi}$ are original and estimated interferometric phases. $T_\psi(\cdot)$ represents the noise reduction process in the complex plane. DWT, using Daubechie's orthogonal wavelet filters, is applied to the real and imaginary parts of the interferometric phase. In the wavelet domain, a complex wavelet coefficient, C_w, is defined, the amplitude and phase of which can be written as:

$$|C_w| = |DWT_n\{\Re(e^{j\psi})\} + j \cdot DWT_n\{\Im(e^{j\psi})\}| \quad (2)$$

$$\arg\{C_w\} = \arg\{DWT_n(\Re(e^{j\psi})) + j \cdot DWT_n(\Im(e^{j\psi}))\} \quad (3)$$

where n indicates the number of scales of the DWT. Phase (eqn. 3) can be defined as a wavelet interferometric phase. This phase has the same information as the interferometric phase ψ, but split in the wavelet scales. The amplitude values (eqn. 2) depend on signal and noise content, being inversely proportional to the noise content. Interferometric noise can be reduced, decreasing the effect of complex wavelet coefficients with low amplitude (eqn. 2).

Complex wavelet coefficients at different scales and giving information about the same area in the original image, can be related using hierarchical relationships between these scales [3]. Due to interferometric phase properties, wavelet complex coefficients at low frequency scales are dominated by useful information, whereas those located at high frequency scales are dominated by noise, i.e. there is a signal concentration at low frequency scales. Wavelet hierarchies are defined over $|C_w|$, and then a signal model is defined within each hierarchy by taking the coefficient with the maximum value, c_{max}, as the useful signal, the remainder being considered as noise. Noise standard deviation σ_n is calculated from the highest frequency scale coefficients. Then, for each hierarchy, a reduction parameter is defined as

$$f_{red} = \alpha \cdot \frac{\sigma_n^2}{c_{max}^2} \quad (4)$$

where α is an adjustment constant (equal for the whole image). f_{red} will depend on signal content, the higher this content the lower its value. As f_{red} will be applied only over $|C_w|$ to those coefficients considered as noise (i.e. coefficients with low amplitude) the effect is to reduce the amplitude of noise coefficients in areas with a signal, and without significantly altering areas dominated by noise. However, since the real and imaginary parts of the transformed phase are processed by the same amount, the relation is maintained, with the consequence that phase is maintained. The result is that the phase of low amplitude coefficients (noise coefficients) will not be incorporated in the inverse transformation process, thereby reducing their contribution to the recovered phase. This reduction will be performed locally, due to DWT. Inverse DWT is applied to the processed real and imaginary parts in the wavelet domain. Denoised phase is then obtained by taking the phase between the real and imaginary processed parts in the original domain.

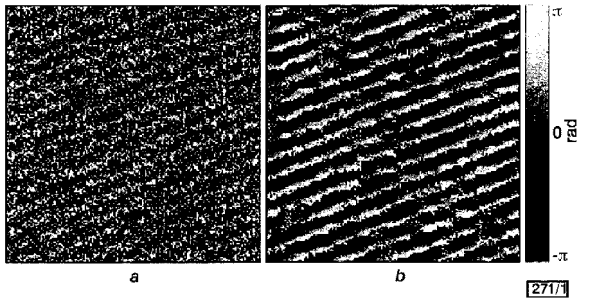

Fig. 1 *Synthetic interferogram (coherence equal to 0.4)*

a Original interferometric phase
b Interferometric phase denoised with proposed algorithm

Results: To test the proposed technique, synthetic and real interferograms have been used. An X-band interferogram of Mount Etna, taken with the German E-SAR, was employed. Synthetic interferograms of a ramp of 512 × 512 pixels, contaminated with phase noise covering the coherence range from 0.1 to 0.95, have been simulated. Fig. 1 shows a detailed image (150 × 150 pixels), making it evident that the proposed algorithm does not create artifacts in the processed image. Fig. 2 shows numerical results (using synthetic interferograms) obtained with the proposed algorithm and with a multilook filter using a 5 × 5 pixels window. For coherences greater than 0.45, the proposed algorithm outperforms the multilook phase filter. For lower coherences (areas with almost only noise), despite obtaining worse numerical results than the multilook filter, the proposed algorithm has the advantage that it hardly alters these areas, avoiding the creation of artifacts or ghost fringes, while maintaining the original resolution.

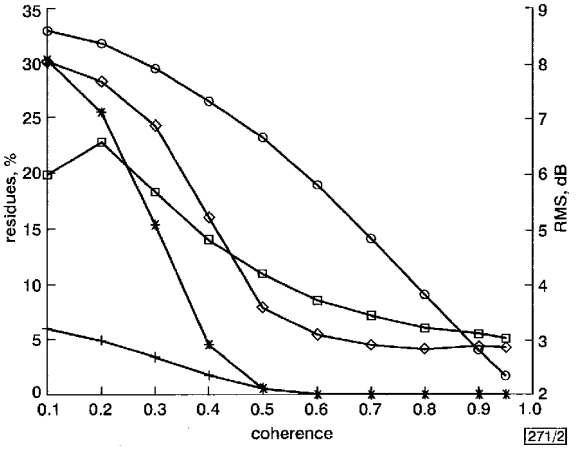

Fig. 2 *Algorithm performance*

○ original interferometric phase residues (%)
+ denoised interferometric phase residues (%) (multilook filter)
✳ denoised interferometric phase residues (%) (proposed algorithm)
□ RMS (dB) between original and denoised interferometric phase (multilook filter)
◇ RMS (dB) between original and denoised interferometric phase (proposed algorithm)

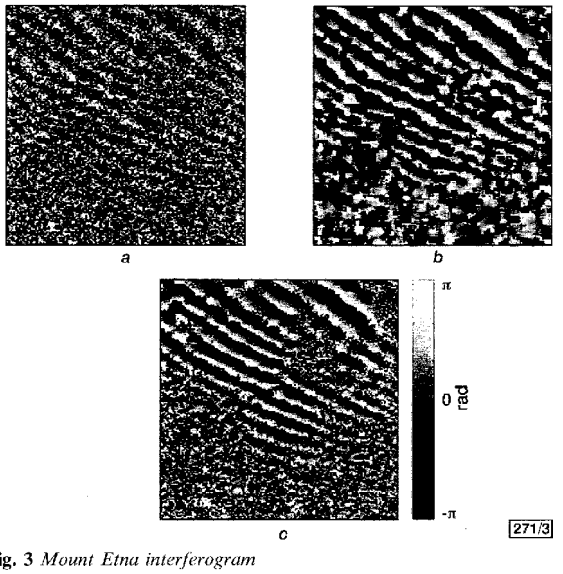

Fig. 3 *Mount Etna interferogram*

a Original interferometric phase
b Processed interferometric phase with multilook filter
c Processed interferometric phase with proposed algorithm

Fig. 3 shows detailed images (150 × 150 pixels) of the Mount Etna interferogram. It is shown that the proposed technique preserves areas containing only noise, and does not lose fringes of the original image. The results shown in Fig. 3 prove that the proposed technique clearly outperforms the multilook filter, overall in

areas containing only noise, and that it almost completely preserves most of the original resolution.

Conclusions: A new technique for SAR interferometric noise reduction, based on the wavelet transform, has been presented. The technique is highly robust in the presence of noise, avoiding the loss of resolution, while preserving the original fringes. The proposed technique provides better results than those obtained using a multilook filter.

5 March 2001
Electronics Letters Online No: 20010438
DOI: 10.1049/el:20010438

C.L. Martínez and M. Chandra (*Institute of Radio Frequency Technology and Radar Systems, German Aerospace Center DLR, Muenchener strasse 20, 82230 Wessling, Germany*)

E-mail: carlos.lopez@dlr.de

X.F. Cànovas (*Signal Theory and Communications Department, Technical University of Catalonia UPC, Jordi Girona 1-3, 08034 Barcelona, Spain*)

References

1 LEE, J.S., PAPATHANASSIOU, K.P., AINSWORTH, T.L., GRUNES, M.R., and REIGBER, A.: 'A new technique for noise filtering of SAR interferometric phase images', *IEEE Trans. Geosci. Remote Sens.*, 1998, **36**, (5), pp. 1456–1465

2 MALLAT, S.: 'A wavelet tour of signal processing' (Academic Press, San Diego, CA, USA, 1999), 2dn edn.

3 SHAPIRO, J.M.: 'Embedded image coding using zerotrees of wavelet coefficients', *IEEE Trans. Signal Process.*, 1993, **41**, (12), pp. 3445–3462

Analysis of Snoop TCP protocol in GPRS system

J. Rendón, F. Casadevall, D. Serarols and J.L. Faner

The General Packet Radio Service system provides an easy adaptation to bursty traffic generated by Internet applications, e.g. e-mail, WWW and FTP. These applications use TCP as the transport protocol and therefore good interaction is necessary between the TCP and GPRS protocols. The performance of the Snoop TCP protocol in a GPRS network is analysed.

Introduction: The General Packet Radio Service (GPRS) is the packet switching data service for GSM. It provides an easy adaptation to the bursty traffic generated by Internet applications, e.g. e-mail, WWW and FTP. All three of these applications use transmission control protocol (TCP) as the transport protocol. TCP is a protocol initially designed for working in fixed networks such as the Internet, where the main problem is congestion. The problems in wireless networks vary: bursty packet losses, high packet delays depending on the wireless network, variable throughput, etc. There have been some proposals which enhance the TCP performance in wireless networks. One of the most well known is the Snoop TCP protocol.

The Snoop TCP protocol [1] consists of having an agent installed at the base station which makes local retransmissions on the wireless paths depending on the type of acknowledgments (ACKs) received from the mobile host (MH) and on local timers. Snoop hides the TCP sender in the fixed host (FH) from losses in the wireless link. When the Snoop agent detects a loss, it retransmits the lost TCP segment to the MH, waits for the corresponding ACK and sends it to the FH before the FH realises there has been a packet loss. Snoop TCP is a protocol which has been proven to work well in a wireless LAN environment [2], but its performance in a mobile cellular network such as GPRS has not been analysed. In this Letter we analyse, with the use of a simulator, the behaviour of the Snoop TCP protocol under realistic conditions in GPRS.

Simulator structure: The GPRS radio link simulation model has been created with the event driven simulator Cadence Bones Designer. We simulate the FTP transmission of a 512Kbytes data file from an FTP server attached to the Internet to a mobile host connected to the GPRS network.

We have simulated the behaviour of all the main nodes that exist in the GPRS architecture. An FTP server, with the corresponding TCP and IP layers, models the fixed host. TCP-Reno version is assumed. The Internet cloud is modelled by means of a loss packet probability and a delay. The delay is statistically characterised as a Gaussian random variable. The GPRS backbone is characterised as follows: the gateway GPRS support node (GGSN) is represented with a router, whereas the serving GPRS support node (SGSN) is modelled as a fixed delay that represents the node process delay. The SGSN node contains the Snoop agent. The GGSN-SGSN and SGSN-BSS (base station subsystem) links are also modelled with fixed delays, which take into account the limited link capacities, i.e. 2Mbit/s and 64Kbit/s, respectively.

In the radio link, a transmission at the logical link control (LLC) layer has been simulated. The LLC layer has been simulated operating in unacknowledged mode. The RLC/MAC layer has been implemented in detail. The MAC layer uses the slotted Aloha access mechanism. A round robin scheduling method without priorities is assumed. The RLC layer uses a selective-repeat ARQ mechanism. In the GPRS radio interface we can vary the number of users, the coding scheme, the channel conditions (C/I), the number of PDCHs, the type of service offered (WWW, FTP or e-mail), and the transmission direction (uplink/downlink). Three types of bursty traffic have been considered in the radio interface, i.e. e-mail, WWW and FTP. We have distributed the type of users in the following form: 50% e-mail, 30% WWW and 20% FTP.

Table 1: Comparison of throughput and retransmissions

	Without Snoop	With Snoop	
Retransmissions	FH	FH	Snoop
	%	%	%
Data-driven	3.0	1.3	12.5
Timer-driven	10.5	21.4	13.1
Total retransmissions	13.5	22.7	25.6
Throughput	1.373Kbit/s	1.053Kbit/s	

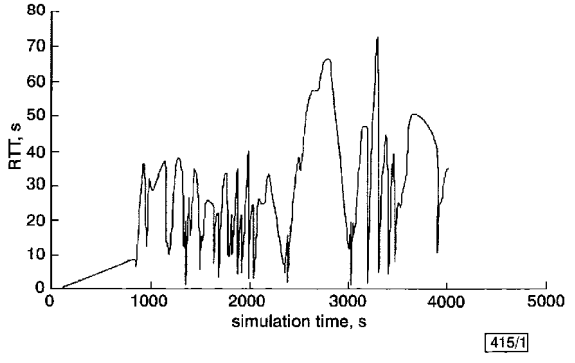

Fig. 1 *RTT (FH), TCP with Snoop*

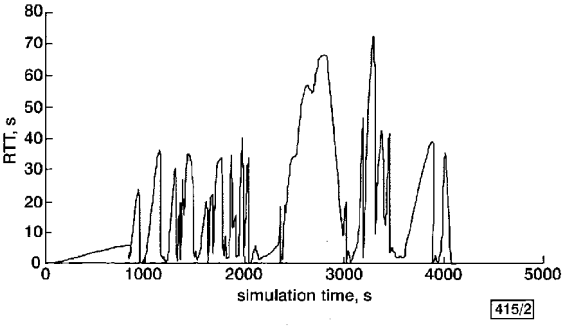

Fig. 2 *RTT (Snoop agent), TCP with Snoop*